ELSEVIER

Catalysis Today 36 (1997) 3–14

CATALYSIS TODAY

Catalytic synthesis of methanol, higher alcohols and ethers

Kamil Klier *, Alessandra Beretta, Qun Sun, Owen C. Feeley, Richard G. Herman

Lehigh University, Department of Chemistry, Seeley G. Mudd Building, 6 East Packer Avenue, Bethlehem, PA 18015-3172, USA

Abstract

Methanol, higher alcohols and ethers are synthesized on a large scale over heterogeneous catalysts with specific functionalities. When copper is the key component of the methanol and higher alcohol catalysts, alkali promotion gives rise to dramatic enhancements of yields due to non-dissociative activation of CO and promotion of aldol coupling with reversal of oxygen retention. Ethers are formed from alcohols over solid acid catalysts, both organic sulfonic resins and inorganic compounds such as zeolites, by a preferential surface S_N2 pathway. This is exemplified by ^{18}O retention in reactions of two different alcohols, chirality inversion where asymmetric carbon is involved, and kinetics that reflect competition of the reactant alcohols for surface acid sites. Transition state shape selectivity is exemplified in the reaction of 2-pentanol and ethanol in H-ZSM-5 and selectivity due to orthogonality of the S_N2 pathway to main channel direction in the formation of dimethyl ether in H-mordenite.

Keywords: Methanol; Higher alcohols; Ethers; Cs promotion; Zeolites; S_N2 reaction

1. Introduction

The overall scheme of alcohol and ether synthesis from a single carbon source is depicted in Fig. 1. Methane reforming or carbon (primarily coal) gasification produces synthesis gas, represented in the figure as CO/H_2 but also containing CO_2, H_2O and impurities, which is followed by the synthesis of methanol and higher alcohols over copper-based, alkali-promoted catalysts. While methanol synthesis from synthesis gas is a large scale industrial process, several other desirable processes are under development or in an experimental stage. Those included in Fig. 1 are: (i) oxidative coupling of methane to C_2 hydrocarbons; (ii) direct oxidation of methane to formaldehyde and methanol; (iii) coupling of alcohols to ethers; and (iv) synthesis of esters, amines, and branched hydrocarbons.

In this paper, we will mainly address alcohol synthesis from CO/H_2 and coupling of alcohols to ethers, some of which have a well-known value as octane enhancers, others are potential cetane enhancers [1], and dimethylether (DME) is of interest in combined energy cycles. Methanol synthesis has been addressed in many patents and papers, and attention to the copper-based catalysts that have become the mainstay of the ICI, Lurgi, and other technologies, has been drawn by Natta in 1955 [2], albeit the invention predates Natta's review. The kinetics are complex [3] and the mechanism does not

* Corresponding author.

PII S0920-5861(96)00190-3

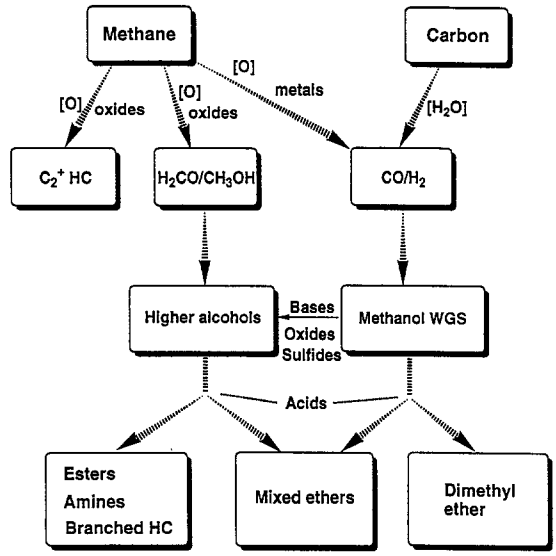

Fig. 1. Processes for the catalytic synthesis of oxygenated fuels and chemicals.

appear to be resolved, although many proposals have been put forward in the literature. What seems to be established is that there is a direct path to hydrogenation of CO_2 [4] as well as of CO [5], the latter being favored in the presence of alkali promoters [6–8] which also accelerate the water gas shift reaction [9,10]. While the role of heavy alkali in promoting methanol synthesis was not recognized before Nunan et al. [6] demonstrated the very large rate enhancement at an optimum surface concentration particularly of cesium promoter, the alkali promotion of higher alcohol synthesis (HAS) has been very well known since the 1930's [11]. There has been a steady progress in understanding the HAS mechanism as well as its kinetic patterns. In the subsequent section, we will give salient examples based on isotopic labeling experiments and will demonstrate how combined understanding of mechanism and kinetics led to a double bed reactor design for enhanced yields of 2-methyl-1-propanol (isobutanol). Further downstream, the alcohols can be dehydratively coupled to ethers over solid acid catalysts, and novel results are presented that show selectivity patterns entirely controlled by the catalysts used.

2. Higher alcohol synthesis: The key role of the aldol step

Before the aldol C–C bond formation can be utilized in the chain growth of higher from lower alcohols, the single carbon source must be converted to a C_2 oxygenate. This can occur by various chemical mechanisms but one usually dominates over another when different catalysts are used. With the alkali-promoted copper-based catalysts, a path that couples two methanol molecules is preferred over the methanol–CO reaction [12]. This is a well-recognized bottleneck step which proceeds at a much slower rate than the subsequent aldol steps involving C_2^+ oxygenated intermediates. The remaining HAS pattern, i.e., the product composition, the isotope flows, the relative rates, and the steric hindrances, is successfully described by a pathway model depicted in Fig. 2 [13]. The pivotal species is a 1,3-keto-alkoxide formed from an enolate and an aldehyde or ketone in the coordination sphere of the alkali cation. Two important subsequent steps are in competition which determines the

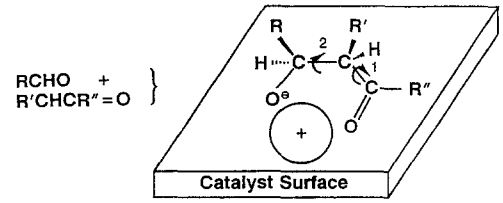

Fig. 2. Representation of the surface intermediate formed during alcohol synthesis via aldol coupling [13]. Strong steric hindrance by bulky R″ and computations that show transition states close to trans-1,3-keto-alkoxide, with E_a (cis → trans) of Cs < Rb < Na, explain the high activity and selectivity of the heavy alkali promoters.

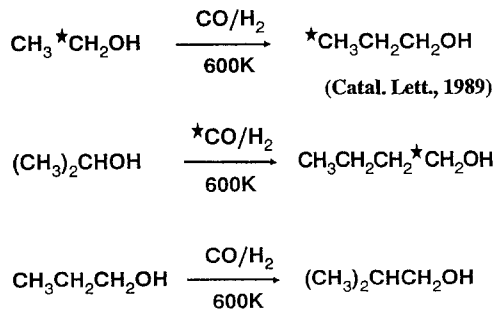

Fig. 3. Aldol pathways with oxygen retention reversal over the Cs/Cu/ZnO catalysts, with * C indicating ^{13}C-labelled carbon atoms.

nature of the product: cis–trans isomerization followed by hydrogenation of the keto group, giving rise to **aldol coupling with oxygen retention reversal** (***R***), and hydrolysis of the alkoxide followed by dehydration/hydrogenation, giving rise to the **normal aldol** (***N***) **product** [13]. Ab initio HF/3-21G calculations elucidate the promotion order Cs > Rb > K > Na in effecting the ***R*** path through lowering of the activation energy for the cis–trans isomerization over the larger cations. The effect is in fact so significant that the ***R*** pathway becomes exclusive when the alkali cation is Cs^+ and cis–trans isomerization is sterically unhindered such as in the $C_2 \rightarrow C_3$ step [14,15]. Three salient

Table 1
The main products in higher alcohol synthesis over the 3 mol% $Cs/Cu/ZnO/Cr_2O_3$ catalyst, the 4 mol% $Cs/ZnO/Cr_2O_3$ catalyst, and the double-bed combination of the two catalysts

	$Cs/Cu/ZnO/Cr_2O_3$ (g/kg cat per h)	$Cs/ZnO/Cr_2O_3$ (g/kg cat per h)	$Cs/Cu/ZnO/Cr_2O_3 + Cs/ZnO/Cr_2O_3$ (g/kg cat per h)
Methanol	1200.0	173.4	178.8
Ethanol	68.7	2.7	7.1
1-Propanol	83.2	11.5	23.5
2-methyl-1-propanol	65.6	74.1	138.8
2-methyl-1-butanol	21.0	8.3	32.9
2-methyl-1-pentanol	14.4	5.3	21.7
2-methyl-1-hexanol	13.5	0.9	24.0
2-methyl-3-pentanol	16.0	5.5	23.1
% CO conversion	11.7	4.5	6.6

Operating conditions:
Single bed 3 mol% $Cs/Cu/ZnO/Cr_2O_3$ (2 g): $T = 598$ K, $P = 7.6$ MPa, $H_2/CO = 0.75$, GHSV = 18375 ℓ(STP)/kg cat per h;
Single bed 4 mol% $Cs/ZnO/Cr_2O_3$ (2 g): $T = 678$ K, $P = 7.6$ MPa, $H_2/CO = 0.75$, GHSV = 18375 ℓ(STP)/kg cat per h; and
Double-bed catalysts consisting of the top-bed = 3 mol% $Cs/Cu/ZnO/Cr_2O_3$ (1 g) at $T = 598$ K and the bottom-bed = 4 mol% $Cs/ZnO/Cr_2O_3$ (1 g) at $T = 678$ K with $H_2/CO = 0.75$ synthesis gas at $P = 7.6$ MPa and GHSV = 18375 ℓ(STP)/kg cat per h.

examples are given in Fig. 3. The first is the highly selective ***R*** pathway in the $C_2 \rightarrow C_3$ chain growth step. The second is the reaction of 2-propanol, not a native product of the synthesis but one that when injected yields 1-butanol by the ***R*** pathway. Because of a steric hindrance due to one of the methyl groups ($R'' = CH_3$ in Fig. 2), the hydrolytic path ***N*** is given time to proceed to some extent to also give rise to 2-butanol [13,15]. The third example in Fig. 3 is the most important step in the formation of isobutanol from 1-propanol, and both the ***R*** and the ***N*** path give rise to the same product. Aldol synthesis does not occur on β-branched aldehydes, and, therefore, isobutanol is a major terminal product. However, higher products are still formed, e.g., by $C_n + C_m$ pathways. The synthesis pattern was cast into successful kinetic models by several groups including our [16], and a full quantitative account was obtained for alcohols and esters up to C_6 products. The same kinetic model was found applicable to the model Cs/Cu/ZnO catalyst, the "real" $Cs/Cu/ZnO/Cr_2O_3$ catalyst, as well as to the copper-free, high temperature alkali/zinc chromate HAS catalyst. The variations in kinetic parameters over different catalysts led Beretta et al. [17] to a double-bed reactor design aimed at enhancement of isobutanol yields. The yields of the key products obtained in this configuration are compared with each single bed catalyst component in Table 1.

3. Coupling of alcohols to ethers

The general pattern of coupling of alcohols to ethers over solid acid catalysts is exemplified in Fig. 4 by reactions of simultaneously present methanol and isobutanol. Both the organic polymeric sulfonic acids and inorganic systems of varying strength and nature of acidity have been investigated in our laboratory. Nunan et al. [18,19] discovered that the main product of methanol–isobutanol reaction over the acid form of Nafion, a synthetic fluorocarbon sulfonic resin, is methyl-isobutyl ether (MIBE) rather than methyl-tertiarybutyl ether (MTBE) which would be expected if carbenium intermediates derived from isobutanol were formed. Nafion in its various forms is a swelling polymer, although the degree of swelling can be somewhat controlled by cross-linking into what has been named Nafion-microsaddles (Nafion-MS). In both cases the internal structure is a cluster-network with narrow openings ($\approx$ 1 nm) between larger cavities in which the backbone-bound $-SO_3^-$ groups

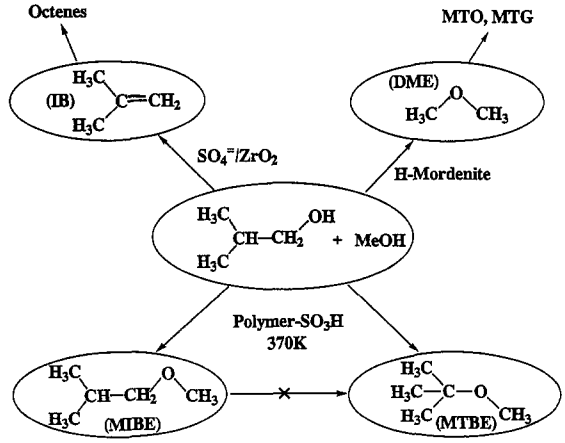

Fig. 4. Pathways for the synthesis of ethers via acid-catalyzed coupling of alcohols, $ROH + R'OH \rightarrow ROR' + H_2O$, and the formation of isobutene, where product selectivity is controlled by the nature (Brönsted–Lewis), strength (super-acid), concentration (for dual site reactions) of acid sites and pocket shape.

Table 2
Activity of polymeric resin catalysts at 90°C and 0.1 MPa with [methanol/isobutanol] = 1:1

Catalyst	% Methanol conversion	% Isobutanol conversion
Nafion-H	1.4	1.4
BioRad AG 50W X-2	4.9	5.4
Purolite C-150	9.2	9.9
Amberlyst-15	9.1	10.2
Amberlyst-1010	5.0	4.2
Amberlyst-35	16.4	15.8
Amberlyst-36	12.3	10.2

carry acidic protons in H – Nafion-MS. The structure is expected to be flexible, certainly under swelling conditions in the presence of intracavital liquid. The narrow connecting channels suggest that diffusion will play an important role when Nafion is used as catalyst. It was, therefore, surprising to find that the alcohol coupling reactions appear to occur in the kinetic regime [19]. The dependence of the rates of formation of MIBE, DME, DIBE, and of isobutanol dehydration to isobutene neatly obeyed Langmuir–Hinshelwood kinetics wherein the two reacting alcohols compete for the acid sites of Nafion-H. At the same time, excess isobutanol self-poisons its dehydration to isobutene, giving rise to high selectivity to MIBE at high pressures [19].

The behavior of other polymeric acid resins is similar to that of Nafion-H, with variations of overall rates (Table 2) and selectivities (Fig. 5) due to different surface concentrations of acid sites and different relative binding strengths of the two reactant alcohols to the acid sites [19,20]. One salient feature of this catalysis by acidic polymeric resins is that the more active Amberlyst-H

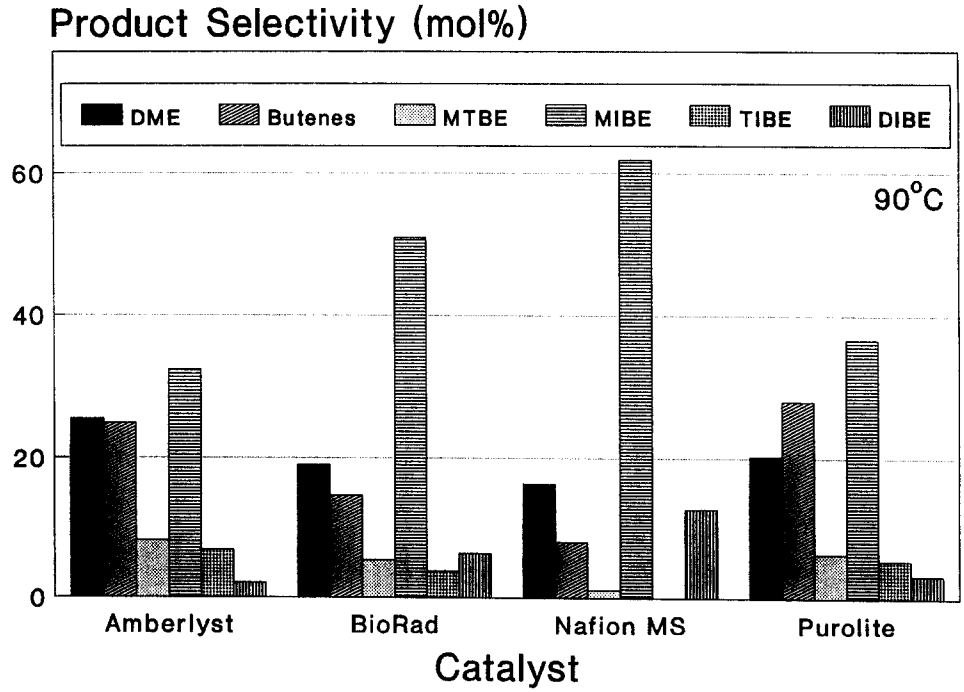

Fig. 5. Product selectivity (mol%) over resin catalysts 5 g at 90°C and 0.1 MPa with methanol = isobutanol = 1.72 mol/kg cat per h in a He/N_2 carrier gas flowing at 16 mol/kg cat per h.

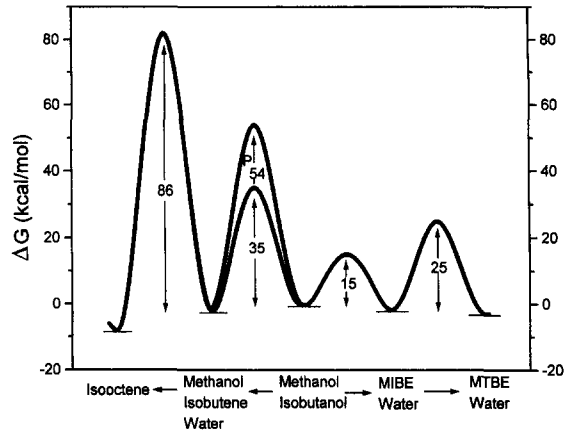

Fig. 6. Thermodynamic and activation energy profiles in methanol/isobutanol reactions over the organic resin Nafion-H MS catalyst at atmospheric pressure with an alcohol partial pressure of 101.3 kPa. For the reaction involving dehydration of isobutanol to isobutene in the mixture of the two alcohols, higher activation energy is found at higher partial pressures, i.e., ≤ 600 kPa.

hydrocarbon sulfonic acids are less selective toward MIBE than Nafion-H. It should be pointed out that MIBE is thermodynamically less favored than its isomer MTBE, and yet MTBE is formed in very small quantities over the acidic polymers used. Apparent activation energy profiles measured over Nafion-H-MS [21] provide an operational explanation: the MIBE formation is the most facile of several possible reactions of methanol and isobutanol, occurring with activation energy of only 15 kcal/mol. A combined thermodynamic and activation energy profile of these reactions is shown in Fig. 6.

There is a very intriguing mechanistic underpinning of the above described kinetic behavior, which was revealed with the use of isotopes and chiral compounds combined with product composition and kinetics, namely that the alcohol coupling is dominated by a dual-site acid-catalyzed S_N^2 reaction. In Fig. 7, results of coupling of ^{16}O-isobutanol with ^{18}O-methanol are shown, giving evidence for different paths to MIBE and MTBE, with a strong indication of S_N2 mechanism for the former and

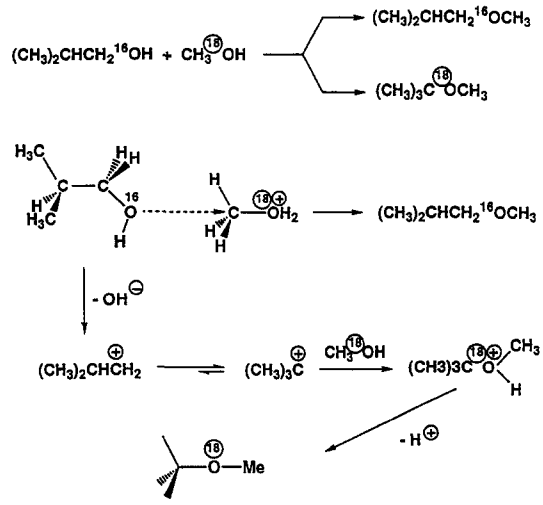

Fig. 7. Selective ^{18}O incorporation indicates sterically hindered S_N2 reaction for MIBE and a carbenium path for MTBE.

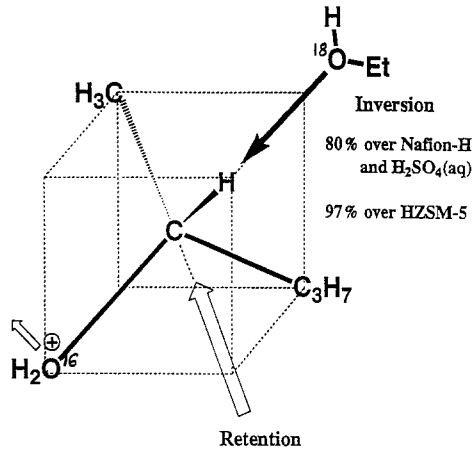

Fig. 8. S_N2 reaction of ethanol and chiral 2-pentanol that results in chiral inversion of the asymmetric carbon in the 2-ethoxypentane product.

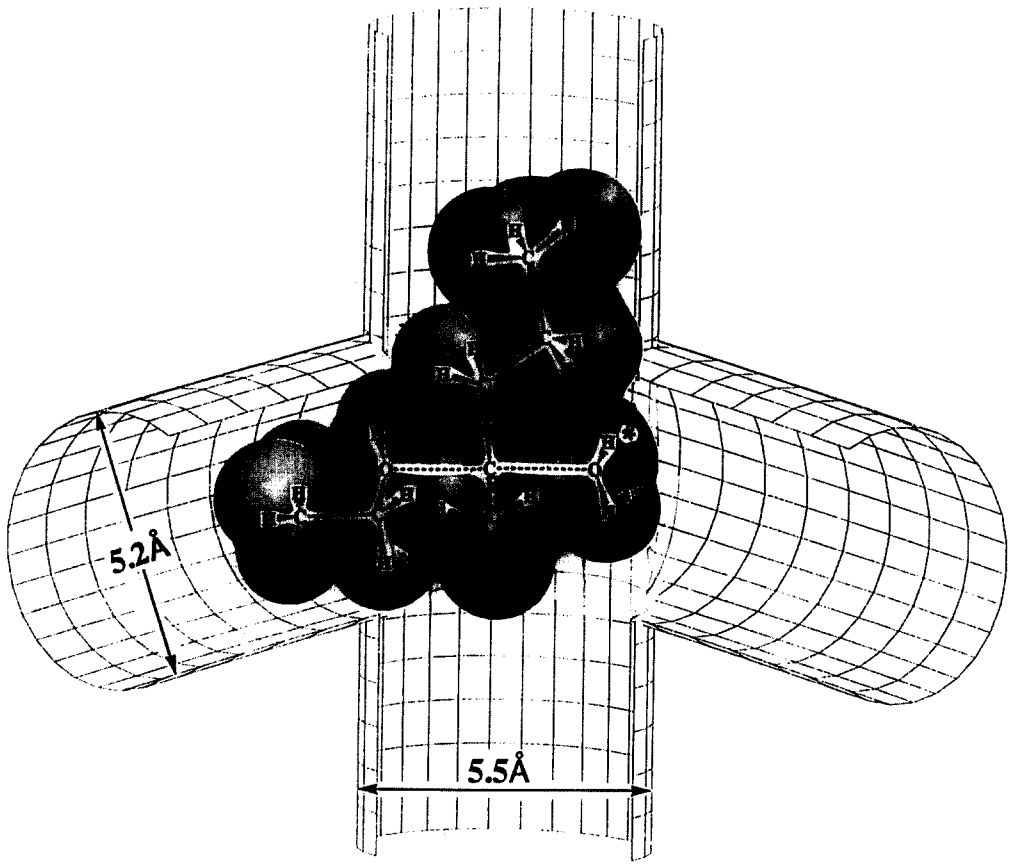

Fig. 9. Transition state complex in the S_N2 reaction of ethanol with chiral 2-pentanol activated by the proton H^* at the channel intersection of ZSM-5 zeolite.

Table 3
Space time yields of the products (mol/kg cat per h) formed over H-mordenite, H-ZSM-5 zeolite, and other inorganic catalysts from methanol = isobutanol = 1.72 mol/kg cat per h reactants in He/N_2 carrier gas at 0.1 MPa as a function of temperature

	$T_{Reaction}$ (°C)	DME	Butenes	MIBE	MTBE	C_8 ether
H-mordenite	90	0.060	–	–	–	–
	125	0.660	–	–	–	–
	150	0.830	0.068	–	–	0.004
H-ZSM-5	90	0.005	0.001	0.012	–	–
	125	0.071	0.169	0.350	0.004	0.003
	150	0.261	0.339	0.134	0.003	0.003
	175	0.185	1.086	0.131	0.005	0.002
Silica–alumina	90	–	–	–	–	–
	125	0.007	0.028	0.011	0.001	0.003
	150	0.021	0.225	0.032	0.005	0.014
	175	0.039	0.943	0.049	0.007	0.016
Montmorillonite	90	–	–	–	–	–
	125	0.008	0.008	0.008	–	0.004
	150	0.019	0.071	0.019	0.004	0.014
	175	0.034	0.378	0.029	0.014	0.003
γ-Alumina	90	–	–	–	–	–
	125	0.006	–	0.007	–	–
	150	0.035	–	0.038	–	–
	175	0.118	0.002	0.160	–	–
	200	0.253	0.023	0.450	–	–
	225	0.342	0.242	0.831	–	–
	250	0.470	1.073	0.493	–	–

carbenium intermediacy for the latter [22]. A final confirmation of the S_N2 mechanism arises from the use of reactants with asymmetric centers which undergo chiral inversion along the S_N2 pathway [23,24]. Sun et al. [25] in this laboratory employed the coupling of S-2-pentanol with ethanol as a mechanistic probe for solid acid catalysts, of both the polymer and inorganic variety (Fig. 8). We observed 78% inversion in the formation of 2-ethoxypentane over Nafion-H, which is comparable to the selectivity obtained in concentrated sulfuric acid [25]. However, when the same reaction was carried out over the H-ZSM-5 zeolite, 97% inversion selectivity was observed due to the shape and space constraints on the transition state at the intersection of the two channel systems of ZSM-5. To assess the effect, the transition-state (TS) geometry was theoretically optimized by using the SPARTAN program at the RHF/STO-3G level forcing the S_N2 pathway to be axial [24] and the zeolite matrix rigid, resulting in the TS structure shown in Fig. 9. Clearly the TS fits tightly into the channel intersection space, indicating that the active zeolite protons are located at the intersection and that side reactions such as the formation of 3-ethoxypentane are excluded. Thus, the S_N2 inversion selectivity in Nafion-H closely resembles that in liquid acid, but a constrained space around the active site in acid zeolite further enhances chiral inversion when the S_N2 transition state is restricted by a "lock and key" type match.

We now turn to the methanol–isobutanol coupling over inorganic catalysts of a wide variety: acid aluminosilicates and sulfated zirconia. Table 3 compares ether and olefin yields over H-mordenite, H-ZSM-5, silica-alumina, montmorillonite and γ-alumina.

Here we concentrate on the remarkable selectivity of H-mordenite to DME with the exclusion of reactions of isobutanol to which the main channels of mordenite (7.0 × 6.5 Å) are freely accessible. On the contrary, ZSM-5 with narrower channels (5.3 × 5.6 Å) allows reactions of isobutanol to yield butenes, MIBE, MTBE, and higher ethers. The selectivity of H-mordenite to DME is attributed to a

Fig. 10. S_N2 reaction of methyl oxonium in the side pocket of mordenite with (A) methanol that results in selective DME formation and (B) isobutanol that is hindered from reacting by the opposing side wall of the main channel.

combination of shape selectivity of the reaction in the side pocket system (entrance dimensions 3.7×4.8 Å) over ''buried'' protons accessible only to methanol to form a side-pocket entrapped methyl oxonium, followed by an S_N2 rear-attack by methanol from the main channel [26]. Computer graphics for this approach based on space-filling Dreiding models for the reactants and Van der Waals dimension-adjusted wireframe model for the mordenite framework is represented in Fig. 10A. A similar approach path for the rear-attack of side-pocket embedded methyl oxonium by isobutanol, depicted in Fig. 10B, demonstrates that this reaction is hindered by isobutanol having to ''turn the corner'' from the axial flight along the main channel to the S_N2 path axis perpendicular to that of the main channel, which disables the formation of MIBE.

While acid zeolites and aluminas catalyze the methanol-isobutanol reaction to the dominant ether product, sulfated zirconia (ZrO_2/SO_4^{2-}) directs the selectivity primarily to isobutene, as shown in Fig. 11. Even at 175°C, almost no methanol was converted to products, while 78.5% of the isobutanol was transformed to products, with the productivity of butenes ($> 85\%$ isobutene) corresponding to 1.29 mol/kg cat per h. This remarkable reaction pattern is no doubt caused by preferential activation of isobutanol, at temperatures above 100°C, over the very strongly acidic sites of the ZrO_2/SO_4^{2-}

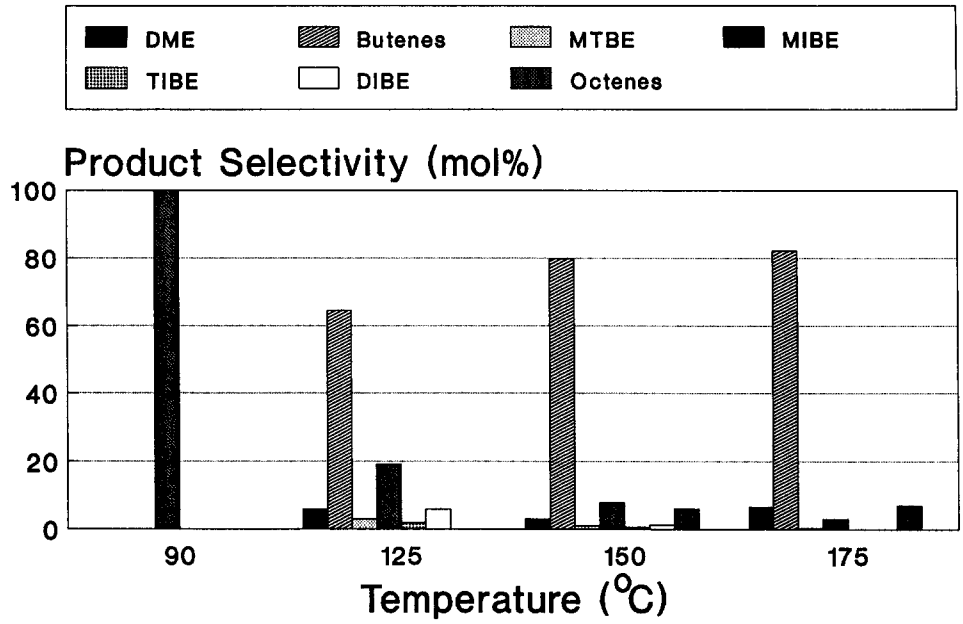

Fig. 11. Product selectivity over ZrO_2/SO_4^{2-} from methanol/isobutanol = 1:1 reactant at 0.1 MPa.

catalyst. Indeed, removing methanol from the reactant stream even further increased the productivity of butenes to 1.44 mol/kg cat per h. The high activity of this catalyst was further demonstrated by increasing the isobutanol flow rate to 20.3 mol/kg cat per h and increasing the reaction temperature to 225°C, whereupon 70.9% of the alcohol was selectively converted to butenes with 79% selectivity to isobutene. The ability of the ZrO_2/SO_4^{2-} catalyst to produce isobutene selectively from methanol-isobutanol mixtures gives perspective to a two-stage process for MTBE from methanol-isobutanol [1], schematically

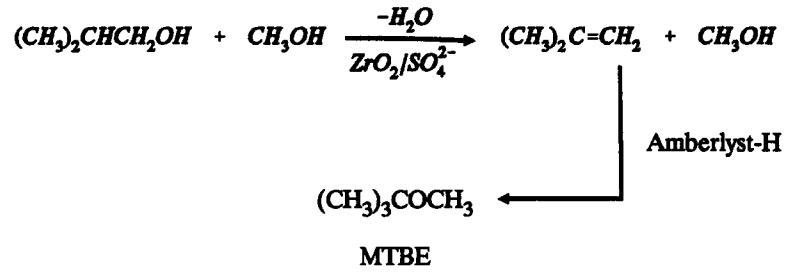

The catalytic chemistry of alcohol coupling to ethers thus offers a variety of pathways that is of both fundamental mechanistic significance and practical value in producing established octane enhancers (MTBE, ETBE, TAME) or potential cetane boosters (MIBE).

4. Conclusions

Recent advances have been made in the development of active and selective catalysts for the synthesis of methanol, higher alcohols, and ethers, and this has been aided by simultaneously

establishing fundamental mechanistic insight into the surface chemistry that directs the synthesis pathways. After demonstrating that Cs promotion of the low temperature Cu/ZnO-based methanol synthesis catalyst switches the selectivity toward isobutanol, a dual catalyst configuration has been employed to enhance the productivity of the methanol/isobutanol product mixture. It was shown that, without optimization studies being completely carried out, that productivity of isobutanol/methanol (in a 1.0/1.3 wt ratio) formed from hydrogen-deficient synthesis gas over a $Cs/Cu/ZnO/Cr_2O_3$ catalyst combined with a high temperature $Cs/ZnO/Cr_2O_3$ catalyst was 0.32 kg/kg cat per h, where the isobutanol component corresponded to 2.5 mol/kg cat per h.

Direct coupling of isobutanol with methanol gave rise to butenes, MIBE, MTBE, and DME in various ratios controlled by the acid catalyst used, e.g., the SO_4^{2-}/ZrO_2 catalyst yielded isobutene selectively while H-mordenite selectively produced DME. The maximum productivity to ethers was that to MIBE (over Amberlyst-35 to produce 1.0 mol/kg cat per h at 117°C and 1.3 MPa) and DME (over H-mordenite to produce 0.83 mol/kg cat per h with 96.6% yield with respect to methanol at 150°C and 0.1 MPa). MTBE was a minor product, with selectivity increasing with decreasing temperature.

It was shown that the SO_4^{2-}/ZrO_2 catalyst was very active and selective in forming isobutene from isobutanol, e.g., an initial productivity as high as 11.4 mol isobutene/kg cat per h (0.64 kg/kg cat per h) at 225°C and 0.1 MPa with this catalyst. By combining this catalyst with a low temperature Amberlyst-15 catalyst in a dual reaction configuration, productivity of 0.35 mol/kg cat per h for MTBE was achieved under unoptimized reaction conditions. These productivities compare with the productivity of MTBE from isobutene + methanol in a commercial process over Amberlyst-15 of 1.1 mol/kg cat per h (0.1 kg/kg cat per h).

Mechanistic understanding of alcohols-to-ethers catalysis has been significantly enhanced by

1. kinetic studies, including effects of water,
2. ^{18}O incorporation experiments and
3. chiral syntheses.

The dual-site concerted S_N2 reaction dominates over the carbenium pathway at low temperatures. This explains the selectivities of MIBE > MTBE and MIBE > DME over some catalysts and of DME > mixed ethers over H-mordenite. There is self-poisoning at high pressure of all catalysts involved in dehydration of isobutanol to isobutene.

Acknowledgements

We thank the US Department of Energy, Pittsburgh Energy Technology Center for partial financial support of this research.

References

[1] R.G. Herman, K. Klier, O.C. Feeley and M.A. Johansson, Preprints, Div. Fuel Chem., Am. Chem. Soc., 39 (1994) 343.
[2] G. Natta, in: P.H. Emmett, Ed., Catalysis, Vol. III, Reinhold, New York, NY, 1955, p. 349.
[3] K. Klier, V. Chatikavanij, R.G. Herman and G.W. Simmons, J. Catal., 74 (1982) 343.
[4] A.Y. Rozovskii, G.I. Lin, L.G. Liberov, E.V. Sliminskii, S.M. Loktev, Y.B. Kagan and A.N. Bashkirov, Kinet. Katal., 18 (1977) 691; V.D. Kuznetsov, F.S. Shub and M.J. Temkin, Kinet. Katal., 23 (1982) 932; G.C. Chinchen, P.J. Denny, D.G. Parker, M.S. Spencer and D.A. Whan, Appl. Catal., 30 (1987) 333.
[5] G.A. Vedage, R. Pitchai, R.G. Herman and K. Klier, Proc. 8th Int. Congress on Catalysis, II, Verlag Chemie, Weinheim, 1984, p. 47.
[6] J. Nunan, K. Klier, C.-W. Young, P.B. Himelfarb and R.G. Herman, J. Chem. Soc., Chem. Commun., (1986) 193.
[7] G.A. Vedage, P. Himelfarb, G.W. Simmons and K. Klier, Am. Chem. Soc. Symp. Ser., 279 (1985) 295.

[8] K. Klier, R.G. Herman and G.A. Vedage, US Patent 4,843,101 (June 27, 1989).
[9] K. Klier, R.G. Herman and G.A. Vedage, US Patent 5,021,233 (June 4, 1991).
[10] K. Klier, C.-W. Young and J.G. Nunan, Ind. Eng. Chem. Fundam., 25 (1986) 36.
[11] G.D. Graves, Ind. Eng. Chem., 23 (1931) 1381.
[12] J.G. Nunan, C.E. Bogdan, K. Klier, K.J. Smith, C.-E. Young and R.G. Herman, J. Catal., 113 (1988) 410.
[13] K. Klier, R.G. Herman, P.B. Himelfarb, C.-W. Young, S. Hou and J.A. Marcos, in: L. Guczi, F. Solymosi and P. Tétényi, Eds., New Frontiers in Catalysis, Stud. Surf. Sci. Catal., Vol. 75, Elsevier and Akadémiai Kiadó, Budapest, Hungary, 1993, p. 1442.
[14] J.G. Nunan, C.E. Bogdan, R.G. Herman and K. Klier, Catal. Lett., 2 (1989) 49.
[15] J.G. Nunan, C.E. Bogdan, K. Klier, K.J. Smith, C.-W. Young and R.G. Herman, J. Catal., 116 (1989) 195.
[16] K.J. Smith, R.G. Herman and K. Klier, Chem. Eng. Sci., 45 (1990) 2639.
[17] A. Beretta, Q. Sun, R.G. Herman and K. Klier, J. Chem. Soc., Chem. Commun., (1995) 2525.
[18] J.G. Nunan, K. Klier and R.G. Herman, J. Chem. Soc., Chem. Commun., (1985) 676.
[19] J.G. Nunan, K. Klier and R.G. Herman, J. Catal., 139 (1993) 406.
[20] L. Lietti, Q. Sun, R.G. Herman and K. Klier, Catal. Today, 27 (1996) 151.
[21] K. Klier, R.G. Herman, R.D. Bastian, S. DeTavernier, M.A. Johansson, M. Kieke and O.C. Feeley, High octane ethers from synthesis gas-derived alcohols, in: G.J. Stiegel and R.D. Srivastava, Eds., Proc. Liquefaction Contractor's Meeting, US Department of Energy, Pittsburgh Energy Technology Center, 1991, pp. 20–49.
[22] O.C. Feeley, Q. Sun, R.G. Herman, M.A. Johansson, L. Lietti and K. Klier, Catal. Lett., 35 (1995) 13.
[23] C.K. Ingold, Structure and Mechanism in Organic Chemistry, 2nd ed., Cornell University Press, Ithaca, NY, 1969, Ch. 7.
[24] S.S. Shaik, H.B. Schlegel and S. Wolfe, Theoretical Aspects of Physical Organic Chemistry: The S_N2 Mechanism, Wiley, New York, NY, 1992.
[25] Q. Sun, R.G. Herman and K. Klier, J. Chem. Soc., Chem. Commun., (1995) 1849.
[26] K. Klier, Q. Sun, O.C. Feeley, M.A. Johansson and R.G. Herman, Stud. Surf. Sci. Catal., 101A (1996) 601.